Tetrahedron 65 (2009) 3042–3051

Contents lists available at ScienceDirect

Tetrahedron

journal homepage: www.elsevier.com/locate/tet

A mechanistic analysis of the Rh-catalyzed intramolecular C–H amination reaction

Kristin Williams Fiori, Christine G. Espino, Benjamin H. Brodsky, J. Du Bois *

Department of Chemistry, Stanford University, Stanford, CA 94305-5080, USA

ARTICLE INFO

Article history:
Received 12 November 2008
Accepted 19 November 2008
Available online 27 November 2008

ABSTRACT

A detailed mechanistic investigation of the intramolecular dirhodium tetracarboxylate-catalyzed sulfamate ester C–H amination reaction is presented. These studies provide support for the formation of a sulfamate-derived iminoiodinane, which reacts rapidly with the rhodium catalyst to generate a nitrenoid-type oxidant. Reactivity patterns, Hammett analysis, kinetic isotope measurement, and a cyclopropane clock experiment are indicative of a concerted, asynchronous transition structure in the product-determining C–H insertion event.

1. Introduction

Recent advances in the design of catalytic methods for the intramolecular amination of C–H bonds have provided unique tools for the synthesis of complex amine-derived products.[1] Such chemistries are marked by their efficiency and selectivity, and conveniently make available several different heterocyclic structures from simple starting materials (Fig. 1).[2,3] In addition to identifying new substrates and advancing new protocols and catalysts for C–H amination, we have engaged in mechanistic studies aimed at revealing the nature of the active oxidant and identifying the steps in the catalytic cycle that precede the C–H insertion event.[4,5] Herein, we provide experimental evidence that supports the following conclusions: (1) the reactive oxidant is best described as a Rh-bound nitrene; (2) C–H functionalization occurs through a concerted, asynchronous pathway; and (3) the requisite condensation between the substrate and terminal oxidant is largely disfavored. These findings have added to our general understanding of metal-mediated C–H amination reactions and have been instrumental for the continued evolution of such methods.

2. Results and discussion

2.1. Reactivity trends

Rhodium-catalyzed C–H amination has been demonstrated to function with carbamate, urea, guanidine, sulfamate, sulfamide, and sulfonamide (not shown) substrates (Fig. 1).[6,7] Due to the general effectiveness of sulfamate esters for C–H insertion, the mechanistic studies described in this work have focused exclusively on reactions with these materials.

In our earliest reports, the stereospecific oxidation of enantioenriched 3° C–H centers was highlighted as a defining characteristic of this method.[3a,e,8] Such a property is suggestive of a mechanism involving the concerted orchestration of C–N bond formation and C–H bond cleavage, in accord with prior work of Müller (Fig. 2).[5a] The stereospecific nature of the amination process is analogous to that of Rh-catalyzed carbene insertion, for which a concerted, asynchronous pathway leading to C–C bond formation is generally accepted.[9,10] Stereospecific modification of a 3° C–H bond, however, is insufficient evidence to discount a stepwise process for oxidation that occurs by initial homolytic C–H abstraction followed by rapid radical rebound.[11] Additional data, including C–H bond reactivity trends, cyclopropane clock experiments, kinetic isotope effect (KIE) measurements, and Hammett analysis are needed to distinguish between these two limiting pathways. Thus, in order to examine in greater detail the sulfamate C–H insertion event, these experiments were performed.

For a reaction such as sulfamate ester oxidation, intramolecular competition experiments offer a straightforward method for delineating the rank order of C–H bond reactivity. Such data are invariant of the reaction kinetics and the rate-limiting step in the catalytic cycle. Accordingly, a series of sulfamate derivatives was prepared having two chemically distinct C–H bonds positioned at

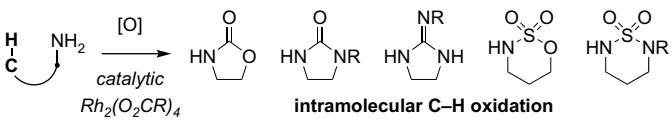

Figure 1. Heterocycle synthesis through Rh-catalyzed C–H amination.

* Corresponding author. Tel.: +1 650 724 4557; fax: +1 650 725 0259.
E-mail address: jdubois@stanford.edu (J. Du Bois).

0040-4020/$ – see front matter © 2008 Published by Elsevier Ltd.
doi:10.1016/j.tet.2008.11.073

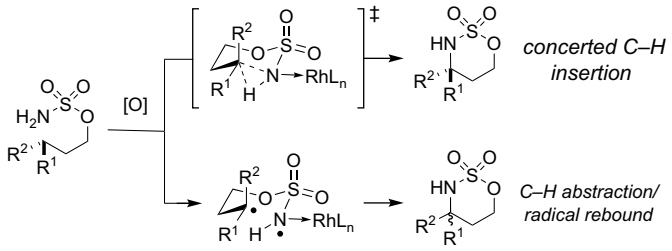

Figure 2. Putative mechanisms for Rh-catalyzed C–H insertion.

the γ and γ′ carbon centers (Table 1). The ratio of the product heterocycles formed in the oxidation reaction is, in effect, a measure of the rate at which each C–H center can engage the active oxidant. These types of experiments can be used to query the influence of substituent effects (steric or electronic) and catalyst structure on chemoselectivity.

Table 1
Catalyst influence on reaction chemoselectivity

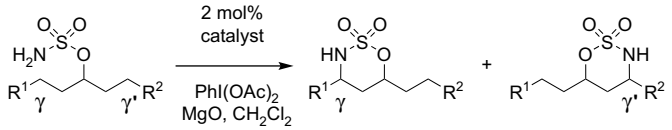

Entry	Substrate	Catalyst[a]	γ/γ′[b]
1	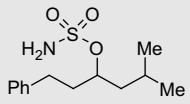	$Rh_2(OAc)_4$	1:1.5
		$Rh_2(O_2C^tBu)_4$	1:1.5
		$Rh_2(esp)_2$	1:7
		$Rh_2(O_2CCPh_3)_4$	1:14
2	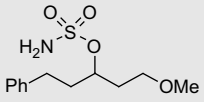	$Rh_2(OAc)_4$	1:1
		$Rh_2(O_2CCPh_3)_4$	1:15
3	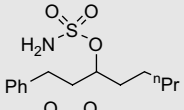	$Rh_2(OAc)_4$	8:1
		$Rh_2(O_2CCPh_3)_4$	1:1.5
4	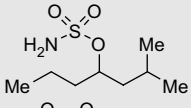	$Rh_2(OAc)_4$	1:20
		$Rh_2(O_2CCPh_3)_4$	1:4.5
5	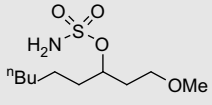	$Rh_2(OAc)_4$	1:11
		$Rh_2(O_2CCPh_3)_4$	1:14
6	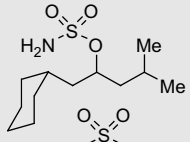	$Rh_2(OAc)_4$	1:2
		$Rh_2(O_2C^tBu)_4$	1:2
		$Rh_2(O_2CCPh_3)_4$	1:6
7	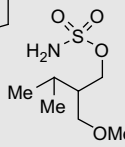	$Rh_2(O_2C^tBu)_4$	1:1
		$Rh_2(O_2CCPh_3)_4$	1:3.5
8	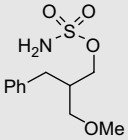	$Rh_2(OAc)_4$	1:3
		$Rh_2(O_2CCPh_3)_4$	1:10

[a] Reactions performed in CH_2Cl_2 at 23 °C using 1.1 equiv of $PhI(OAc)_2$, 2.3 equiv of MgO, and 2 mol % of the indicated catalyst.
[b] Product ratios are based on integration of the ^1H NMR spectrum of the unpurified reaction mixture and are not corrected for statistics.

Each sulfamate ester in Table 1 was subjected to oxidative cyclization using 2 mol % of a dimeric Rh(II)-tetracarboxylate catalyst ($Rh_2(OAc)_4$, $Rh_2(O_2C^tBu)_4$, $Rh_2(esp)_2$, $Rh_2(O_2CCPh_3)_4$), 1.1 equiv of $PhI(OAc)_2$, and MgO.[12,13] In all cases, oxathiazinane heterocycles were formed exclusively and neither of the five-membered ring sulfamidates was obtained. Product ratios were determined by ^1H NMR analysis of the unpurified material and, as is apparent from these findings, selectivity for the two oxathiazinane isomers varied dramatically depending on the catalyst employed. Comparing the information gathered from experiments with $Rh_2(OAc)_4$, a qualitative rate scale for C–H amination can be drawn as follows: 3°>ethereal ~ benzylic>2°>>1°. Primary methyl C–H bonds are at the bottom end of the reactivity spectrum and, in fact, we have witnessed in only one rare example the product of $-CH_3$ insertion. Three additional observations merit comment: (1) general reactivity trends parallel those observed in Rh-catalyzed carbenoid insertions; (2) the connectivity of the sulfamate can effect the product outcome albeit to a small, yet still discernible, degree (cf. entries 2 and 8); and (3) the catalyst structure can influence product selectivity. This latter point has important mechanistic implications and provides the most compelling evidence for an active oxidant that is Rh-bound. Results with $Rh_2(O_2CCPh_3)_4$ are striking in this regard (for example, entries 1, 2, 3, and 5) and suggest that remote steric effects between the substrate and catalyst framework can be employed to direct reaction chemoselectivity.[14,15] As a general rule, insertion at benzylic centers is strongly disfavored in reactions promoted by $Rh_2(O_2CCPh_3)_4$.[16,17]

As the same oxidative protocols for C–H bond amination serve effectively for olefin aziridination, the matter of chemoselectivity in cyclization reactions of unsaturated sulfamates manifests.[18] A small collection of differentially configured alkene substrates was fashioned to examine this question (Table 2). In three cases (entries 1–3), C–H oxidation could occur at an allylic center to give the corresponding oxathiazinane product. Alkene aziridination, on the other hand, would afford a fused 7,3-bicyclic ring system. As indicated by these collective data, aziridination is, at a minimum,

Table 2
C–H insertion versus alkene aziridination

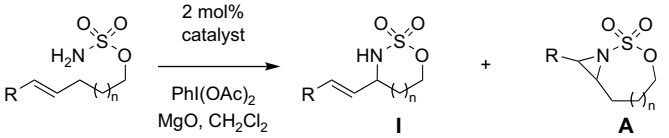

Entry	Substrate	Catalyst[a]	I/A[b]
1	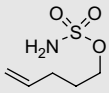	$Rh_2(OAc)_4$	1:1
		$Rh_2(esp)_2$	1:1.5
		$Rh_2(O_2CCPh_3)_4$	1:20
		$Rh_2(NHCOCF_3)_4$	1:4
2	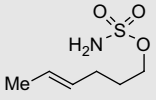	$Rh_2(OAc)_4$	2:1
		$Rh_2(esp)_2$	1:1
		$Rh_2(O_2CCPh_3)_4$	1:5
		$Rh_2(NHCOCF_3)_4$	1:2
3	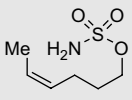	$Rh_2(OAc)_4$	1:1
		$Rh_2(esp)_2$	1:2.5
		$Rh_2(O_2CCPh_3)_4$	1:20
		$Rh_2(NHCOCF_3)_4$	1:4
4	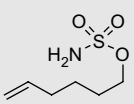	$Rh_2(OAc)_4$	1:1
		$Rh_2(esp)_2$	1:1
		$Rh_2(O_2CCPh_3)_4$	1:7

[a] Reactions performed in CH_2Cl_2 at 23 °C using 1.1 equiv of $PhI(OAc)_2$, 2.3 equiv of MgO, and 2 mol % of the indicated catalyst.
[b] Product ratios are based on integration of the ^1H NMR spectrum of the unpurified reaction mixture.

competitive with allylic amination.[19] Only in one case, which utilizes $Rh_2(OAc)_4$ as catalyst, is a slight bias noted for the six-membered oxathiazinane product (entry 2). In agreement with earlier findings, different catalysts alter product ratios in these types of competition experiments. For reasons not entirely apparent, reactions performed with $Rh_2(O_2CCPh_3)_4$ are strongly biased toward alkene aziridination. Remarkably, the predilection for alkene oxidation by $Rh_2(O_2CCPh_3)_4$ is manifest even in the tris-homoallylic sulfamate (entry 4), a reaction that affords an unusual eight-membered ring bicycle.[20] It is worth noting that oxidation of *cis*- and *trans*-alkene derivatives (entries 2 and 3) is stereospecific, as would be expected for a concerted, electrophilic oxidation process.

Homoallylic sulfamate **1** presents an alternative type of competition substrate for assessing reactivity differences between an alkene and a C–H bond (Fig. 3). With this starting material, all four catalysts employed favor aziridine production, $Rh_2(O_2CCPh_3)_4$ affording the highest degree of selectivity. In these experiments, small changes in the diastereochemical outcome of the aziridination event as a function of catalyst structure are also noted.

The results from competition studies highlighted in Tables 1 and 2 and Figure 3 should provide a useful guide for future substrate designs. Clear reactivity differences between sp^3 C–H bonds exist that are attributable to electronic effects (vide infra); however, the influence of steric forces between substrate and catalyst can be quite pronounced and will, in many cases, supersede intrinsic electronic biases. Next generation catalyst designs will seek to exploit this knowledge. Altogether, the general trends in reactivity between C=C and σ-C–H bonds appear to mirror largely those of Rh-promoted diazoalkene processes, and intimate that the reactive oxidizing species are indeed analogous (i.e., Rh-bound carbene vs Rh-bound nitrene).[9] Hammett analysis, KIE data, and cyclopropane clock studies, as described below, support such speculation.

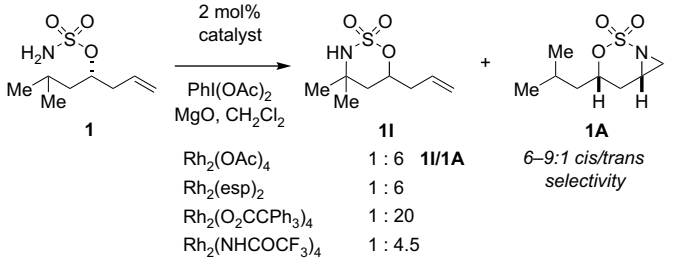

Figure 3. Alkene aziridination out-competes 3° C–H bond insertion.

2.2. Hammett studies

The electronic nature of the transition structure for C–H amination was further investigated by conducting intramolecular competition experiments with substituted diaryl derivatives **2** (Fig. 4).[21] Selectivity for oxidation of one of the two sets of benzylic C–H bonds occurs in the product-determining step and thus the ratio of isomeric oxathiazinanes offers a direct measure of k_{Ar}/k_{Ph}. The advantage of performing a Hammett analysis in this manner is that it renders any prior knowledge of the reaction kinetics unnecessary (i.e., which step is rate-determining step). Accordingly, sulfamates having two electronically disparate benzylic sites suitably disposed for oxathiazinane formation were subjected to $Rh_2(oct)_4$-catalyzed oxidation.[22] Product ratios were evaluated by ^1H NMR integration of the spectra taken on unpurified material and by HPLC analysis, and from this data $\log(k_{Ar}/k_{Ph})$ was determined. Plotting these values against σ^+ parameters for each substituent gives a calculated ρ-value of −0.55.[23] Such a small, negative number is consistent with a picture of the transition structure having some

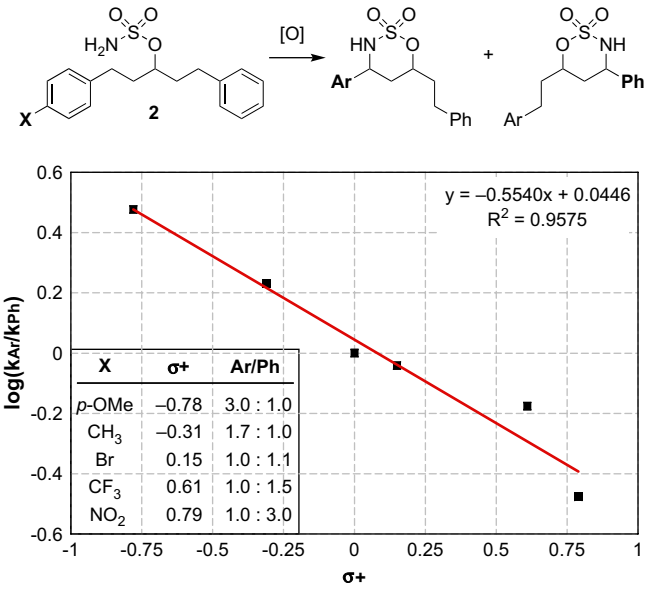

Figure 4. Hammett analysis of $Rh_2(oct)_4$-catalyzed C–H amination.

degree of partial positive charge at the reacting carbon center. An improved fit of the data against σ^+ rather than σ_p values indicates that cationic charge stabilization (δ^+) at the carbon undergoing oxidation is due in part to a resonance contribution.[24] Such findings correlate nicely with our observed reactivity trends. Notably, the calculated ρ-value is similar to that measured in both our lab and Müller's for intermolecular C–H amination (ρ=−0.73 and −0.90, respectively)[4,5a,b] and for both intra- and intermolecular Rh-catalyzed carbene insertion (ρ=−0.78 and −1.27, respectively).[21,25] Hammett analysis of the sulfamate oxidation reaction is thus in accord with an asynchronous, concerted transition structure, as proposed for Rh-carbenoid C–H insertion.[9,10]

2.3. Kinetic isotope effect and radical-clock studies

The measured kinetic isotope effect (KIE) for the Rh-catalyzed amination reaction provides additional support for a concerted oxidation event. As with the Hammett analysis, the magnitude of the KIE was easily determined through an intramolecular competition experiment. Mono-deuterated sulfamate **3** was prepared and when subjected to cyclization under $Rh_2(OAc)_4$ catalysis yielded a 1.9±0.2:1 ratio of oxathiazinane heterocycles (Fig. 5). Analysis of the product mixture by ^{13}C NMR provided the most straightforward and reproducible method for establishing this value.[26] A KIE of 1.9±0.2 is comparable to those found for rhodium-catalyzed carbene C–H insertion reactions, determined to be between 1.2 and 2.1 depending on the catalyst and substrate employed.[27] Additionally, carbethoxynitrene (generated upon base treatment of *N*-(*p*-nitrobenzenesulfonoxy)urethane) reacts with an equimolar mixture of cyclohexane and cyclohexane-d_{12} to give a KIE=1.5±0.2.[28] By contrast, Ru-based intermolecular C–H amination methods, which are generally thought to occur by way of a radical-rebound

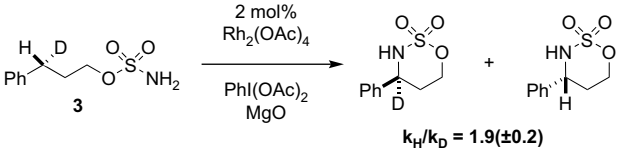

Figure 5. Kinetic isotope effect measured in competition experiment.

mechanism, furnish KIEs of 6–12.[5c,e,29] A recent theoretical analysis of our related carbamate insertion reaction supports a three-centered transition structure for the nitrenoid insertion event.[30–32]

Rhodium-catalyzed amination with a cyclopropyl clock-derived sulfamate provides the final, and arguably the most compelling, piece of evidence to differentiate between a radical-rebound process and a concerted, asynchronous insertion event.[33] Guided by work of Newcomb, phenyl-substituted cyclopropane **4** was prepared (Fig. 6).[11a] The choice of this particular clock follows from a report that describes reactions of dimethyldioxirane with (*trans*-2-phenylcyclopropyl)ethane.[34] The absence of cyclopropane ring opening in such experiments argues for a concerted C–H hydroxylation event. Based on these data, we assume that the rate constant for fragmentation of the cyclopropylcarbinyl radical derived from **4** is on the order of 7×10^{10} s^{-1}.[35] If a C–H abstraction/radical-rebound mechanism was operative in the Rh-catalyzed process, the lifetime of the putative radical would have to be exceedingly short (~200 fs). In both the intramolecular cyclization of **4** and in a related intermolecular C–H amination reaction, we have observed none of the olefin-containing products that would be expected from cyclopropane fragmentation.[4] Although it is possible to employ radical clocks that fragment/rearrange at faster rates, we feel that this data together with the Hammett ρ-value and KIE strongly implicate a concerted, asynchronous pathway for C–H insertion in the Rh-catalyzed amination process.

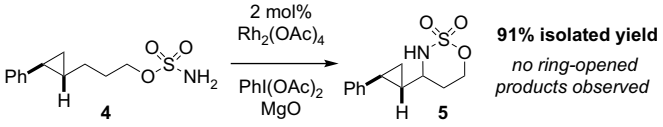

Figure 6. C–H amination of a radical-clock containing substrate.

2.4. Kinetics analysis

Having examined the reactivity properties of the oxidizing species, we wished to understand the detailed steps leading to the formation of this intermediate. Competition experiments performed with equimolar amounts of sulfamates **6** and **8** yielded a 1:1 mixture of the two oxathiazinanes (Fig. 7), in stark contrast to the 20:1 selectivity recorded for intramolecular 3° versus 2° C–H oxidation (see entry 4, Table 1). The disparity between the inter- and intramolecular competition reactions indicates that the rate-determining step (rds) in this catalytic process occurs prior to C–H insertion.

We have analyzed the kinetic order of the catalyst, substrate, and $PhI(OAc)_2$ by measuring reaction rates as a function of concentration for each starting material. In these studies, reactions were performed at 23 °C in CH_2Cl_2 or CD_2Cl_2 using isoamyl sulfamate **10**, $Rh_2(O_2C^tBu)_4$, and $PhI(OAc)_2$ in the absence of any added MgO (Fig. 8). There are several advantages to this set of reaction conditions for mechanistic inquiry, foremost of which is that oxidation of **10** proceeds to high conversion (>90%) without having to include an insoluble salt, MgO.[36] In addition, $Rh_2(O_2C^tBu)_4$ has excellent solubility in halogenated solvents. As such, the time course of the homogeneous reaction could be monitored using ^1H NMR spectroscopy. To ensure the accuracy of these measurements, product formation was also analyzed by quenching small aliquots of the reaction mixture and determining reaction conversion by HPLC.

Initial rates for C–H amination were investigated over a 10-fold catalyst concentration range (0.5–5.0 mol %), data for which are shown in Figure 8. In these experiments, a solution of oxidant was added in a single charge to a mixture of catalyst and sulfamate. The

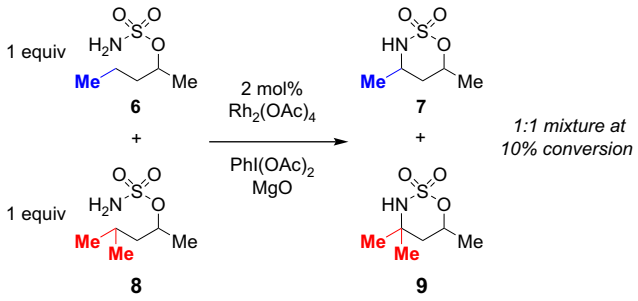

Figure 7. Competition results show that C–H insertion is not the rds.

first data point, measured within 40 s of initiating the reaction, shows ~10% product formation. Remarkably, all five runs at disparate catalyst loads afforded an identical amount of oxathiazinane **11** between 30 and 100 s. While increasing the amount of $Rh_2(O_2{}^tBu)_4$ did improve overall conversion, the data are quite clear that this process is zero order in catalyst in the initial reaction burst.[37]

Further kinetic experiments were conducted to establish the dependence of the reaction rate on substrate concentration. Catalyst loading was fixed at 2 mol % (with respect to $PhI(OAc)_2$) and [**10**] was varied between 0.0785 M and 0.55 M.[38] Observed rate constants (k_{obs}) were determined at each substrate concentration using data recorded between 5 s and 35 s of initiating the reaction. Each trial was repeated twice and an average k_{obs} value was calculated. A plot of k_{obs} versus substrate concentration gives a straight line, indicative of reaction having first-order dependence on sulfamate **10** (Fig. 9).

Our attempts to measure reaction rates as a function of oxidant concentration were, at first, unsuccessful. It appears that deleterious side reactions occur when [$PhI(OAc)_2$] exceeding 0.17 M is used to conduct the amination reaction. Thus, an accurate assessment of the product conversion over a wide enough [$PhI(OAc)_2$] could not be made. Instead, reactions were performed under pseudo-first-order conditions by employing a ninefold excess of substrate **10** and by recording the formation of product **11** over the reaction course. Plotting ln([substrate]/[substrate]$_0$) versus time yielded a straight

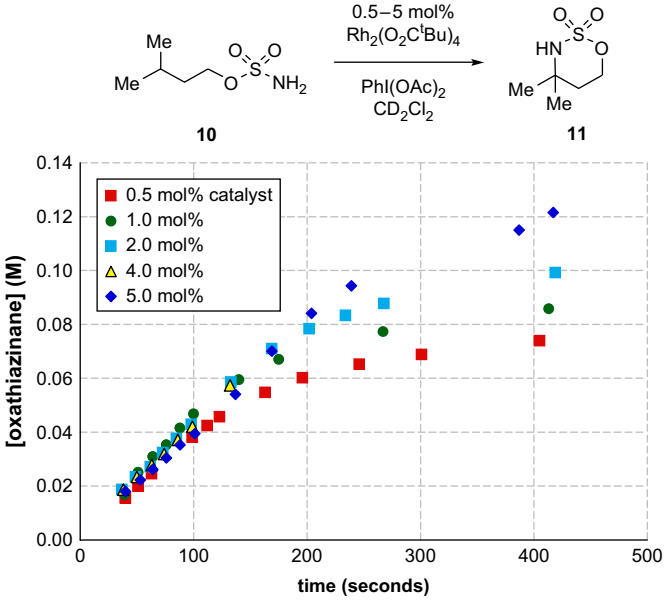

Figure 8. Oxathiazinane **11** formation versus time at different catalyst loadings.

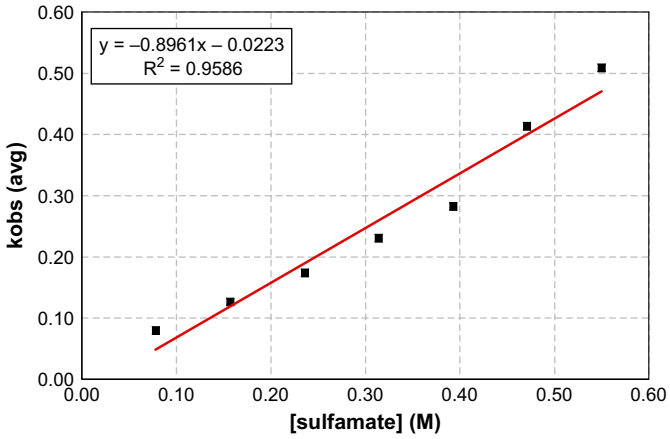

Figure 9. Reaction rate has first-order dependence on [sulfamate].

line for each of the three trials, thereby confirming that reaction rates have a first-order dependence on oxidant.

From the kinetic studies, an initial rate law for the C–H amination reaction may be drawn as, rate=k[substrate]^1[oxidant]^1[catalyst]^0. One possible mechanism that conforms to this rate expression is depicted in Figure 10. Generation of a substrate·oxidant complex could take on several forms including iminoiodinane **12**. Presumably, under the conditions of the reaction, a small amount of **12** is generated and reacts rapidly with the Rh catalyst. Such a scenario is consistent with a zero-order dependence of $Rh_2(O_2C^tBu)_4$ on the initial reaction rate. Several questions arise from this mechanistic postulate: (1) is the iminoiodinane **12** a chemically competent intermediate on the catalytic pathway for C–H insertion; (2) is such an intermediate observable upon mixing sulfamate and oxidant; (3) what is the rate-limiting step in the production of **12**? We have prepared, isolated, and characterized iminoiodinane **15** and have demonstrated that this species does indeed react rapidly (<30 s at 23 °C) with 2 mol % $Rh_2(OAc)_4$ to give the corresponding oxathiazinane (>95% conversion, Fig. 11).[39] Such a finding is not surprising in light of earlier work by Müller using NsN=IPh for Rh-catalyzed intermolecular C–H amination.[5a,b] The inability to observe any of **15** in a CD_2Cl_2 solution of sulfamate **14** and $PhI(OAc)_2$ was, however, quite unexpected. Apparently, the equilibrium between **14**+ $PhI(OAc)_2$→**15** (or an intermediate species) greatly favors the reactants and none of the iminoiodinane is detectable within the limits of ^{1}H NMR.[40,41] The addition of PhSMe to this mixture results in the gradual formation (~24 h) of sulfylimine **17**, thus providing an indirect confirmation for the generation of iminoiodinane under these reaction conditions (Fig. 11).[42] Although it is reasonable to speculate that $Rh_2(O_2CR)_4$ could promote the formation of **15** (by activating the oxidant, for example), its zero-order dependence in the rate law does not accord with such a proposal.

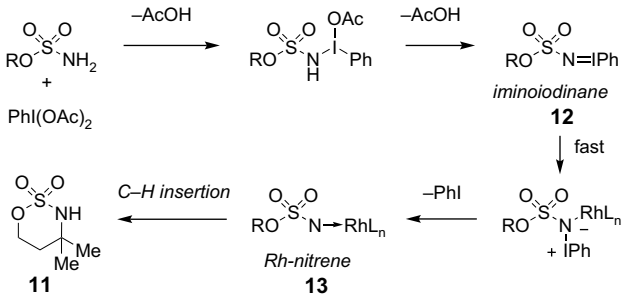

Figure 10. Proposed mechanism for Rh-nitrene formation.

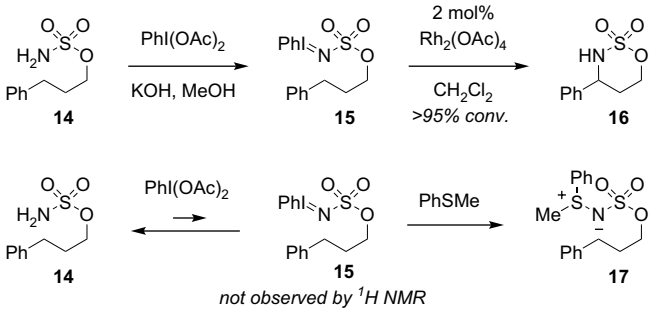

Figure 11. Control experiments with iminoiodinane starting material.

At present, our analysis of the reaction mechanism has been unable to identify the specific rate-determining step in the catalytic reaction cycle. Despite the absence of observable amounts of iminoiodinane **15** in control experiments, its intermediacy is strongly inferred from the recorded data. We note, however, that it is possible to draw more than one path by which **15** may be generated and that an intermediate substrate·oxidant complex may be an equally competent reactant under the reaction conditions. Assuming for now that iminoiodinane **15** is indeed formed, its coordination to the Rh center must be fast relative to its reversion to starting material (or an intermediate species) in order to account for the zero-order dependence of $[Rh_2(O_2CR)_4]$ on the initial reaction rate. Following the first 60–100 s, we speculate that the increasing concentration of RCO_2H must increase the rate of iminoiodinane protonolysis (i.e., **15**→**14**) so as to alter the initial, simplified rate expression. A change in the concentration of active catalyst is also likely responsible for the kinetics data recorded in Figure 8.[2e,43] Further investigations are warranted to assess additional details of this complex reaction process.

3. Conclusions

Rhodium-catalyzed intramolecular C–H amination represents a general method for the preparation of amine-derived heterocycles. Our interest in understanding reactivity trends and other phenomena associated with this process has driven our efforts to dissect the reaction mechanism. A combination of data collected through the use of substrate probes and competition experiments leads to the conclusion that the active oxidizing species is best described as a Rh-bound nitrene and that C–H insertion is likely a concerted, asynchronous event. Reaction kinetics analysis has resulted in the unexpected discovery that the initial rate of product formation is independent of catalyst concentration. This result has led us to postulate a mechanism in which the formation of a sulfamate·oxidant complex (i.e., an iminoiodinane) is rate limiting in the initial reaction burst. The details of the events that ensue beyond the initiation of the amination reaction are most intriguing; unraveling these mysteries should reveal clues for evolving further C–H amination technology.

4. Experimental procedures

4.1. General

All reagents were obtained commercially unless otherwise noted. Reactions were performed using oven-dried glassware under an atmosphere of nitrogen. Air and moisture sensitive liquids and solutions were transferred via syringe or stainless steel cannula. Organic solutions were concentrated under reduced pressure (ca. 15 mmHg) by rotary evaporation. Dichloromethane and acetonitrile were freshly distilled from CaH_2 immediately prior to use. *N*,*N*-Dimethylacetamide

(DMA) was dried over 4 Å molecular sieves and stored under an atmosphere of nitrogen. Chromatographic purification of products was accomplished using forced-flow chromatography on EM Science Geduran silica gel 60 (35–75 μm). Thin-layer chromatography (TLC) was performed on EM Science silica gel 60 F_{254} plates (250 μm). Visualization of the developed chromatogram was accomplished by fluorescence quenching and by staining with ethanolic anisaldehyde, aqueous potassium permanganate, or aqueous ceric ammonium molybdate (CAM) solution. Product melting points were acquired on a Thomas Hoover Capillary Melting Point apparatus.

Nuclear magnetic resonance (NMR) spectra were acquired on a Varian Mercury spectrometer operating at 400 and 100 MHz for ^{1}H and ^{13}C, respectively, or on a Varian Inova spectrometer operating at 500 and 125 MHz for ^{1}H and ^{13}C, respectively, and are referenced internally according to residual solvent signals. Data for ^{1}H NMR are recorded as follows: chemical shift (δ, ppm), multiplicity (s, singlet; br s, broad singlet; d, doublet; br d, broad doublet; t, triplet; q, quartet; quint, quintet; sept, septet; m, multiplet), integration, coupling constant (Hz). Data for ^{13}C NMR are reported in terms of chemical shift (δ, ppm). Infrared spectra were recorded on a Thermo Nicolet IR300 spectrometer and are reported in terms of frequency of absorption. Sample preparation was done either as a thin film on a NaCl salt plate or as a KBr pellet. High-resolution mass spectra were obtained from the Vincent Coates Foundation Mass Spectrometry Laboratory at Stanford University.

4.2. Experimental procedure and characterization data for sulfamate esters (Tables 1 and 2)

4.2.1. General procedure

Formic acid (283 μL, 7.5 mmol, 2.5 equiv) was added to neat $ClSO_2NCO$ (653 μL, 7.5 mmol, 2.5 equiv) at 0 °C with rapid stirring. Vigorous gas evolution was observed during the addition process and within 5 min the mixture solidified. To the resulting white mass was added 6.0 mL of CH_3CN and the contents were then warmed to 23 °C. After stirring for 8 h, the mixture was cooled to 0 °C and a solution of alcohol (3.0 mmol) in 5 mL of DMA was added via cannula. Transfer of the alcohol was made quantitative with an additional 2×0.5 mL of DMA. The reaction was warmed to 23 °C and stirred at this temperature until TLC indicated complete consumption of starting material (~1 h). The reaction mixture was quenched by the addition of 20 mL of H_2O and poured into a separatory funnel containing 75 mL of Et_2O. The organic phase was collected and the aqueous layer was extracted with 2×50 mL of Et_2O. The combined organic extracts were washed with 5×20 mL of H_2O, dried over $MgSO_4$, and concentrated under reduced pressure. Purification of the oily residue by chromatography on silica gel (conditions given below) afforded the desired product.

4.2.1.1. 5-Methyl-1-phenylhexan-3-yl sulfamate (Table 1, entry 1). Purified by chromatography on silica gel (4:1 hexanes/EtOAc); white solid (70%): TLC R_f=0.54 (1:1 hexanes/EtOAc); ^{1}H NMR ($CDCl_3$, 400 MHz) δ 7.32–7.27 (m, 2H), 7.22–7.18 (m, 3H), 4.75–4.68 (m, 1H), 4.68 (br s, 2H), 2.80–2.70 (m, 2H), 2.12–2.00 (m, 2H), 1.81–1.70 (m, 2H), 1.51 (ddd, 1H, J=16.0, 9.8, 5.7 Hz), 0.95 (d, 3H, J=6.4 Hz), 0.93 (d, 3H, J=6.4 Hz) ppm; ^{13}C NMR ($CDCl_3$, 100 MHz) δ 141.1, 128.5, 128.4, 126.1, 83.8, 43.2, 36.0, 31.0, 24.4, 22.7, 22.4 ppm; IR (thin film) ν 3285, 2958, 2870, 1558, 1496, 1455, 1358, 1182, 920, 750 cm^{-1}; HRMS (ES$^+$) calcd for $C_{13}H_{21}NO_3S$ 271.1242, found 294.1138 (MNa^+).

4.2.1.2. 1-Methoxy-5-phenylpentan-3-yl sulfamate (Table 1, entry 2). Purified by chromatography on silica gel (2:1 hexanes/EtOAc); colorless oil (73%): TLC R_f=0.54 (1:1 hexanes/EtOAc); ^{1}H NMR ($CDCl_3$, 400 MHz) δ 7.32–7.27 (m, 2H), 7.22–7.17 (m, 3H), 4.89 (br s, 2H), 4.82–4.75 (m, 1H), 3.59 (ddd, 1H, J=10.1, 6.8, 5.2 Hz), 3.49 (dt, 1H, J=10.1, 5.6 Hz), 3.34 (s, 3H), 2.83–2.69 (m, 2H), 2.14–1.94 (m, 4H) ppm; ^{13}C NMR ($CDCl_3$, 100 MHz) δ 141.0, 128.5, 128.4, 126.1, 81.7, 68.3, 58.5, 36.5, 34.1, 31.1 ppm; IR (thin film) ν 3276, 2931, 1496, 1455, 1361, 1180, 1108, 917 cm^{-1}; HRMS (ES$^+$) calcd for $C_{12}H_{19}NO_4S$ 273.1035, found 296.0938 (MNa^+).

4.2.1.3. 1-Phenyloctan-3-yl sulfamate (Table 1, entry 3). Purified by chromatography on silica gel (4:1 hexanes/EtOAc); white solid (75%): TLC R_f=0.21 (4:1 hexanes/EtOAc); ^{1}H NMR ($CDCl_3$, 400 MHz) δ 7.33–7.26 (m, 2H), 7.23–7.18 (m, 3H), 4.81 (br s, 2H), 4.64 (quint, 1H, J=6.0 Hz), 2.81–2.67 (m, 2H), 2.08–2.01 (m, 2H), 1.82–1.69 (m, 2H), 1.42–1.24 (m, 6H), 0.89 (t, 3H, J=6.8 Hz) ppm; ^{13}C NMR ($CDCl_3$, 100 MHz) δ 141.1, 128.5, 128.3, 126.1, 84.7, 35.5, 34.0, 31.5, 31.1, 24.4, 22.4, 14.0 ppm; IR (thin film) ν 3374, 3285, 3063, 3028, 2955, 2931, 2862, 1706, 1603, 1556, 1496, 1455, 1359, 1183, 1031, 919, 801 cm^{-1}; HRMS (ES$^+$) calcd for $C_{14}H_{23}NO_3S$ 285.1399, found 308.1298 (MNa^+).

4.2.1.4. 2-Methylheptan-4-yl sulfamate (Table 1, entry 4). Purified by chromatography on silica gel (5:1 hexanes/EtOAc); white solid (73%): TLC R_f=0.22 (4:1 hexanes/EtOAc); ^{1}H NMR ($CDCl_3$, 400 MHz) δ 5.13 (br s, 2H), 4.67–4.61 (m, 1H), 1.78–1.62 (m, 4H), 1.47–1.34 (m, 3H), 0.95–0.90 (m, 9H) ppm; ^{13}C NMR ($CDCl_3$, 100 MHz) δ 83.8, 43.1, 36.5, 24.3, 22.8, 22.4, 17.9, 13.9 ppm; IR (thin film) ν 3375, 3287, 2961, 2875, 1559, 1468, 1359, 1184, 921 cm^{-1}.

4.2.1.5. 1-Methoxynonan-3-yl sulfamate (Table 1, entry 5). Purified by chromatography on silica gel (2:1 hexanes/EtOAc); colorless oil (70%): TLC R_f=0.36 (2:1 hexanes/EtOAc); ^{1}H NMR ($CDCl_3$, 400 MHz) δ 4.99 (br s, 2H), 4.72 (quint, 1H, J=6.1 Hz), 3.57 (dt, 1H, J=9.9, 6.5 Hz), 3.47 (dt, 1H, J=9.9, 5.6 Hz), 3.41 (s, 3H), 1.95 (q, 2H, J=6.0 Hz), 1.80–1.65 (m, 2H), 1.42–1.24 (m, 8H), 0.88 (t, 3H, J=6.9 Hz) ppm; ^{13}C NMR ($CDCl_3$, 100 MHz) δ 82.3, 68.4, 58.5, 34.9, 33.9, 31.6, 29.0, 24.7, 22.5, 14.0 ppm; IR (thin film) ν 3283, 3110, 2930, 2860, 1563, 1464, 1366, 1183, 1115, 922, 760 cm^{-1}; HRMS (ES$^+$) calcd for $C_{10}H_{23}NO_4S$ 253.1348, found 276.1253 (MNa^+).

4.2.1.6. 1-Cyclohexyl-4-methylpentan-2-yl sulfamate (Table 1, entry 6). Purified by chromatography on silica gel (4:1 hexanes/EtOAc); white solid (90%): TLC R_f=0.28 (4:1 hexanes/EtOAc); ^{1}H NMR ($CDCl_3$, 400 MHz) δ 4.79–4.72 (m, 1H), 4.69 (br s, 2H), 1.78–1.60 (m, 4H), 1.52–1.40 (m, 2H), 1.31–1.12 (m, 10H), 0.95 (d, 3H, J=6.4 Hz), 0.93 (d, 3H, J=6.4 Hz) ppm; ^{13}C NMR ($CDCl_3$, 100 MHz) δ 82.5, 43.8, 42.3, 33.8, 33.4, 33.1, 26.4, 26.1, 26.1, 24.5, 22.7, 22.4 ppm; IR (thin film) ν 3282, 2925, 2852, 1561, 1449, 1360, 1182, 921, 761 cm^{-1}; HRMS (ES$^+$) calcd for $C_{12}H_{25}NO_3S$ 263.1555, found 286.1450 (MNa^+).

4.2.1.7. 2-(Methoxymethyl)-3-methylbutyl sulfamate (Table 1, entry 7). Purified by chromatography on silica gel (gradient elution: 2:1 → 1:1 hexanes/EtOAc); pale yellow oil (73%): TLC R_f=0.51 (1:1 hexanes/EtOAc); ^{1}H NMR ($CDCl_3$, 400 MHz) δ 5.27 (br s, 2H), 4.27 (dd, 1H, J=9.6, 4.8 Hz), 4.23 (dd, 1H, J=9.6, 5.4 Hz), 3.45 (dd, 1H, J=9.6, 4.4 Hz), 3.37 (dd, 1H, J=9.6, 7.2 Hz), 3.32 (s, 3H), 1.84–1.75 (m, 2H), 0.95 (d, 3H, J=8.8 Hz), 0.93 (d, 3H, J=8.8 Hz) ppm; ^{13}C NMR ($CDCl_3$, 100 MHz) δ 70.4, 70.0, 58.7, 44.0, 26.3, 20.0, 19.8 ppm; IR (thin film) ν 3281, 3107, 2964, 1566, 1467, 1368, 1183, 1113, 931, 832 cm^{-1}; HRMS (ES$^+$) calcd for $C_7H_{17}NO_4S$ 211.0878, found 234.0771 (MNa^+).

4.2.1.8. 2-Benzyl-3-methoxypropyl sulfamate (Table 1, entry 8). Purified by chromatography on silica gel (gradient elution: 2:1 → 1:1 hexanes/EtOAc); white solid (75%): TLC R_f=0.25 (2:1 hexanes/EtOAc); mp 51–53 °C; ^{1}H NMR ($CDCl_3$, 400 MHz) δ 7.32–7.27 (m, 2H), 7.24–7.16 (m, 3H), 5.01 (br s, 2H), 4.21 (dd, 1H, J=9.6, 5.2 Hz), 4.17 (dd, 1H, J=9.6, 5.34 Hz), 3.37 (dd, 1H, J=9.6, 4.9 Hz), 3.33 (dd, 1H, J=9.6, 6.6 Hz), 3.32 (s, 3H), 2.72 (dd, 1H, J=9.6, 5.2 Hz), 2.68 (dd, 1H, J=9.6, 5.3 Hz), 2.32–2.24 (m, 1H) ppm; ^{13}C NMR ($CDCl_3$, 100 MHz) δ 138.8, 129.1, 128.5, 126.4, 71.2, 70.7, 58.8, 40.3,

33.9 ppm; IR (thin film) ν 3367, 3282, 2931, 1560, 1496, 1455, 1368, 1183, 1092, 933, 823 cm^{-1}; HRMS (ES^+) calcd for $C_{11}H_{17}NO_4S$ 259.0878, found 282.0775 (MNa^+).

4.2.1.9. Pent-4-enyl sulfamate (Table 2, entry 1). Purified by chromatography on silica gel (gradient elution: 4:1→2:1 hexanes/EtOAc); colorless oil (77%): TLC R_f=0.37 (2:1 hexanes/EtOAc); ^1H NMR ($CDCl_3$, 400 MHz) δ 5.84–5.74 (m, 1H), 5.10–5.01 (m, 2H), 4.74 (br s, 2H), 4.23 (t, 2H, J=6.4 Hz), 2.22–2.16 (m, 2H), 1.86 (dq, 2H, J=7.9, 6.5 Hz) ppm; ^{13}C NMR ($CDCl_3$, 100 MHz) δ 136.7, 115.9, 70.7, 29.4, 27.8 ppm; IR (thin film) ν 3381, 3287, 3081, 2978, 1642, 1560, 1470, 1446, 1366, 1181, 978, 925, 823 cm^{-1}; HRMS (ES^+) calcd for $C_5H_{11}NO_3S$ 165.0460, found 188.0355 (MNa^+).

4.2.1.10. (E)-Hex-4-enyl sulfamate (Table 2, entry 2). Purified by chromatography on silica gel (gradient elution: 4:1→2:1 hexanes/EtOAc); colorless oil (88%): TLC R_f=0.32 (2:1 hexanes/EtOAc); ^1H NMR ($CDCl_3$, 400 MHz) δ 5.53–5.44 (m, 1H), 5.42–5.34 (m, 1H), 4.69 (br s, 2H), 4.21 (t, 2H, J=6.4 Hz), 2.14–2.08 (m, 2H), 1.80 (dq, 2H, J=7.6, 6.4 Hz), 1.65 (dq, 3H, J=6.2, 1.3 Hz) ppm; ^{13}C NMR ($CDCl_3$, 100 MHz) δ 129.1, 126.6, 70.9, 28.5, 28.3, 17.9 ppm; IR (thin film) ν 3378, 3286, 2940, 2855, 1558, 1449, 1362, 1180, 1072, 968, 938, 824 cm^{-1}; HRMS (ES^+) calcd for $C_6H_{13}NO_3S$ 179.0616, found 202.0513 (MNa^+).

4.2.1.11. (Z)-Hex-4-enyl sulfamate (Table 2, entry 3). Purified by chromatography on silica gel (2:1 hexanes/EtOAc); colorless oil (76%): TLC R_f=0.53 (1:1 hexanes/EtOAc); ^1H NMR ($CDCl_3$, 400 MHz) δ 5.57–5.48 (m, 1H), 5.39–5.31 (m, 1H), 4.78 (br s, 2H), 4.22 (t, 2H, J=6.6 Hz), 2.18 (q, 2H, J=7.3 Hz), 1.82 (dq, 2H, J=7.8, 6.6 Hz), 1.62 (ddt, 3H, J=6.7, 1.8, 0.9 Hz) ppm; ^{13}C NMR ($CDCl_3$, 100 MHz) δ 128.3, 125.6, 70.9, 28.5, 22.6, 12.8 ppm; IR (thin film) ν 3379, 3286, 3015, 2942, 1555, 1444, 1365, 1180, 1058, 939, 823 cm^{-1}; HRMS (ES^+) calcd for $C_6H_{13}NO_3S$ 179.0616, found 202.0512 (MNa^+).

4.2.1.12. Hex-5-enyl sulfamate (Table 2, entry 4). Purified by chromatography on silica gel (gradient elution: 4:1→2:1 hexanes/EtOAc); colorless oil (82%): TLC R_f=0.35 (2:1 hexanes/EtOAc); ^1H NMR ($CDCl_3$, 400 MHz) δ 5.84–5.73 (m, 1H), 5.06–4.96 (m, 2H), 4.81 (br s, 2H), 4.22 (t, 2H, J=6.6 Hz), 2.13–2.06 (m, 2H), 1.80–1.72 (m, 2H), 1.56–1.48 (m, 2H) ppm; ^{13}C NMR ($CDCl_3$, 100 MHz) δ 137.9, 115.2, 71.4, 33.0, 28.1, 24.6 ppm; IR (thin film) ν 3378, 3283, 3078, 2938, 2863, 1640, 1559, 1361, 1179, 917 cm^{-1}; HRMS (ES^+) calcd for $C_6H_{13}NO_3S$ 179.0616, found 178.0531 (M^+-H).

4.2.1.13. (±)-6-Methylhept-1-en-4-yl sulfamate (Fig. 3). Purified by chromatography on silica gel (4:1 hexanes/EtOAc); colorless oil (71%): TLC R_f=0.49 (2:1 hexanes/EtOAc); ^1H NMR ($CDCl_3$, 400 MHz) δ 5.87–5.76 (m, 1H), 5.18–5.12 (m, 2H), 4.81 (br s, 2H), 4.71 (dq, 1H, J=8.4, 5.4 Hz), 2.58–2.44 (m, 2H), 1.82–1.73 (m, 1H), 1.72–1.63 (m, 1H), 1.42 (ddd, 1H, J=14.3, 8.3, 4.9 Hz), 0.94 (d, 3H, J=6.6 Hz), 0.93 (d, 3H, J=6.6 Hz) ppm; ^{13}C NMR ($CDCl_3$, 100 MHz) δ 132.7, 118.8, 82.6, 42.9, 39.1, 24.2, 22.9, 22.1 ppm; IR (thin film) ν 3370, 3284, 2958, 2927, 2871, 1711, 1561, 1468, 1367, 1183, 920, 773 cm^{-1}; HRMS (ES^+) calcd for $C_8H_{17}NO_3S$ 207.0929, found 230.0825 (MNa^+).

4.3. Experimental procedure and characterization data for C–H insertion products (Tables 1 and 2)

4.3.1. General procedure

To a solution of sulfamate ester (0.25 mmol) in 1.6 mL of CH_2Cl_2 were added sequentially MgO (23 mg, 0.57 mmol, 2.3 equiv), $PhI(OAc)_2$ (89 mg, 0.28 mmol, 1.1 equiv), and Rh catalyst (2 mol % of either $Rh_2(OAc)_4$, $Rh_2(O_2CCMe_3)_4$, $Rh_2(esp)_2$,[12] $Rh_2(HNCOCF_3)_4$, or $Rh_2(O_2CCPh_3)_4$, as indicated in Tables 1 and 2). The bright green/blue suspension was stirred vigorously at 23 °C until TLC indicated the complete consumption of starting material (1–12 h). The reaction was filtered through a small pad of $MgSO_4$ and the filter cake rinsed with 2×2 mL of CH_2Cl_2. Purification of the isolated material by chromatography on silica gel (conditions given below) afforded the desired product.

4.3.1.1. cis-4-Phenyl-6-(2-methylpropyl)tetrahydro-1,2,3-oxathiazine-2,2-dioxide (Table 1, entry 1). Purified by chromatography on silica gel (9:1 hexanes/EtOAc); white solid: TLC R_f=0.41 (4:1 hexanes/EtOAc); ^1H NMR ($CDCl_3$, 400 MHz) δ 7.43–7.32 (m, 5H), 4.95 (dddd, 1H, J=11.3, 9.1, 4.2, 2.2 Hz), 4.81 (ddd, 1H, J=12.1, 9.3, 2.8 Hz), 4.22 (br d, 1H, J=9.1 Hz), 2.04 (dt, 1H, J=14.3, 2.6 Hz), 1.95–1.85 (m, 1H), 1.88 (dt, 1H, J=14.3, 11.8 Hz), 1.79 (ddd, 1H, J=14.3, 8.8, 5.5 Hz), 1.44 (ddd, 1H, J=14.0, 8.6, 4.2 Hz), 0.97 (d, 3H, J=6.6 Hz), 0.95 (d, 3H, J=6.7 Hz) ppm; ^{13}C NMR ($CDCl_3$, 100 MHz) δ 138.1, 129.1, 128.9, 126.3, 82.8, 58.3, 44.1, 36.7, 23.8, 22.7, 21.8 ppm; IR (thin film) ν 3266, 2959, 2872, 1498, 1456, 1416, 1362, 1242, 1190, 1075, 1050, 1012, 913, 876, 843, 780 cm^{-1}; HRMS (ES^+) calcd for $C_{13}H_{19}NO_3S$ 269.1086, found 292.0983 (MNa^+).

4.3.1.2. trans-4-Phenyl-6-(2-methylpropyl)tetrahydro-1,2,3-oxathiazine-2,2-dioxide (Table 1, entry 1). Clear oil: TLC R_f=0.34 (4:1 hexanes/EtOAc); ^1H NMR ($CDCl_3$, 400 MHz) δ 7.44–7.33 (m, 5H), 4.98–4.88 (m, 2H), 4.44 (br d, 1H, J=8.4 Hz), 2.39 (ddd, 1H, J=14.3, 9.1, 5.1 Hz), 2.22 (ddd, 1H, J=14.3, 9.9, 5.5 Hz), 2.07 (ddd, 1H, J=14.5, 5.5, 4.4 Hz), 1.97–1.86 (m, 1H), 1.43 (ddd, 1H, J=14.2, 8.7, 4.8 Hz), 0.98 (d, 3H, J=6.6 Hz), 0.97 (d, 3H, J=6.6 Hz) ppm; ^{13}C NMR ($CDCl_3$, 100 MHz) δ 138.1, 129.0, 128.5, 126.3, 82.2, 55.3, 42.5, 29.7, 24.3, 22.9, 21.6 ppm; IR (thin film) ν 3266, 2959, 2926, 2872, 1456, 1417, 1362, 1190, 1089, 1050, 1012, 914, 876, 843, 781 cm^{-1}; HRMS (ES^+) calcd for $C_{13}H_{19}NO_3S$ 269.1086, found 292.0981 (MNa^+).

4.3.1.3. 4,4-Dimethyl-6-(2-phenylethyl)tetrahydro-1,2,3-oxathiazine-2,2-dioxide (Table 1, entry 1). White solid: TLC R_f=0.28 (4:1 hexanes/EtOAc); ^1H NMR ($CDCl_3$, 400 MHz) δ 7.33–7.28 (m, 2H), 7.24–7.18 (m, 3H), 4.84 (dddd, 1H, J=8.6, 7.8, 6.0, 4.0 Hz), 4.01 (br s, 2H), 2.86 (ddd, 1H, J=13.9, 9.6, 5.0 Hz), 2.75 (ddd, 1H, J=13.9, 9.2, 7.2 Hz), 2.07 (dddd, 1H, J=14.2, 9.0, 9.0, 5.2 Hz), 1.88 (dddd, 1H, J=14.2, 9.6, 7.2, 4.0 Hz), 1.47 (s, 3H), 1.30 (s, 3H) ppm; ^{13}C NMR ($CDCl_3$, 100 MHz) δ 140.5, 128.6, 128.5, 126.3, 80.2, 55.9, 41.6, 37.1, 32.0, 30.7, 25.1 ppm; IR (thin film) ν 3267, 3027, 2952, 1496, 1455, 1420, 1389, 1373, 1350, 1192, 1161, 1028, 940, 872, 817 cm^{-1}; HRMS (ES^+) calcd for $C_{13}H_{19}NO_3S$ 269.1086, found 292.0986 (MNa^+).

4.3.1.4. cis-4-Phenyl-6-(2-methoxyethyl)tetrahydro-1,2,3-oxathiazine-2,2-dioxide (Table 1, entry 2). Purified by chromatography on silica gel (2:1 hexanes/EtOAc); white solid: TLC R_f=0.56 (1:1 hexanes/EtOAc); ^1H NMR ($CDCl_3$, 400 MHz) δ 7.43–7.33 (m, 5H), 5.06 (dddd, 1H, J=12.0, 8.0, 4.7, 2.1 Hz), 4.82 (ddd, 1H, J=12.1, 9.1, 2.8 Hz), 4.15 (br d, 1H, J=9.1 Hz), 3.59–3.49 (m, 2H), 3.35 (s, 3H), 2.13 (dt, 1H, J=14.4, 2.5 Hz), 2.09–1.89 (m, 3H) ppm; ^{13}C NMR ($CDCl_3$, 100 MHz) δ 138.0, 129.2, 128.9, 126.3, 81.7, 67.4, 58.9, 58.2, 36.3, 35.5 ppm; IR (thin film) ν 3253, 2923, 1497, 1456, 1420, 1363, 1189, 1116, 1065, 1017, 914, 875, 849 cm^{-1}; HRMS (ES^+) calcd for $C_{12}H_{17}NO_4S$ 271.0878, found 294.0775 (MNa^+).

4.3.1.5. cis-4-Phenyl-6-pentyltetrahydro-1,2,3-oxathiazine-2,2-dioxide (Table 1, entry 3). Purified by chromatography on silica gel (gradient elution: 9:1→4:1 hexanes/EtOAc); white solid: TLC R_f=0.44 (4:1 hexanes/EtOAc); ^1H NMR ($CDCl_3$, 400 MHz) δ 7.42–7.32 (m, 5H), 4.90–4.82 (m, 1H), 4.81–4.74 (m, 1H), 4.43 (br d, 1H, J=9.6 Hz), 2.04 (dt, 1H, J=14.3, 2.6 Hz), 1.92 (dt, 1H, J=14.3, 11.9 Hz), 1.85–1.75 (m, 1H), 1.71–1.62 (m, 1H), 1.56–1.24 (m, 6H), 0.90 (t, 3H, J=6.9 Hz) ppm; ^{13}C NMR ($CDCl_3$, 100 MHz) δ 138.1, 129.0, 128.7, 126.3, 84.4, 58.3, 36.2,

35.1, 31.2, 24.1, 22.4, 13.9 ppm; IR (thin film) ν 3266, 2956, 2932, 2862, 1499, 1456, 1417, 1363, 1190, 1091, 1055, 1014, 912, 876, 795, 753 cm^{-1}; HRMS (ES^+) calcd for $C_{14}H_{21}NO_3S$ 283.1242, found 306.1142 (MNa^+).

4.3.1.6. 4-Propyl-6-(2-phenylethyl)tetrahydro-1,2,3-oxathiazine-2,2-dioxide (Table 1, entry 3). Purified by chromatography on silica gel (gradient elution: 9:1→4:1 hexanes/EtOAc); colorless oil: TLC R_f=0.27 (4:1 hexanes/EtOAc); ^1H NMR ($CDCl_3$, 400 MHz) δ 7.33–7.27 (m, 2H), 7.24–7.18 (m, 3H), 4.82 (sept, 1H, J=4.3 Hz), 4.22 (br d, 1H, J=7.6 Hz), 3.68–3.60 (m, 1H), 2.88 (ddd, 1H, J=14.0, 9.1, 5.1 Hz), 2.73 (ddd, 1H, J=14.0, 9.1, 7.4 Hz), 2.36–2.26 (m, 1H), 1.94–1.84 (m, 3H), 1.68 (ddd, 1H, J=14.4, 5.6, 4.0 Hz), 1.58–1.42 (m, 2H), 1.42–1.31 (m, 1H), 0.93 (t, 3H, J=7.2 Hz) ppm; ^{13}C NMR ($CDCl_3$, 100 MHz) δ 140.5, 128.6, 128.5, 126.2, 81.6, 53.3, 36.3, 35.3, 33.5, 31.1, 19.3, 13.6 ppm; IR (thin film) ν 3273, 2959, 2933, 2871, 1455, 1420, 1375, 1184, 913, 869, 811 cm^{-1}; HRMS (ES^+) calcd for $C_{14}H_{21}NO_3S$ 283.1242, found 306.1148 (MNa^+).

4.3.1.7. 4,4-Dimethyl-6-propyltetrahydro-1,2,3-oxathiazine-2,2-dioxide (Table 1, entry 4). Purified by chromatography on silica gel (6:1 CH_2Cl_2/hexanes); white solid: TLC R_f=0.26 (10:1 CH_2Cl_2/EtOAc); ^1H NMR ($CDCl_3$, 400 MHz) δ 4.82–4.76 (m, 1H), 4.49 (br s, 1H), 1.75–1.64 (m, 1H), 1.62–1.35 (m, 5H), 1.44 (s, 3H), 1.26 (s, 3H), 0.91 (t, 3H, J=7.3 Hz) ppm; ^{13}C NMR ($CDCl_3$, 100 MHz) δ 81.0, 55.8, 41.4, 37.2, 31.8, 25.1, 17.8, 13.6 ppm; IR (thin film) ν 3266, 2963, 2876, 1466, 1422, 1351, 1193, 1157, 1005, 945, 878, 801 cm^{-1}; HRMS (EI) calcd for $C_8H_{17}NSO_3$ 207.0929, found 208.1013 (MH^+).

4.3.1.8. 4-(2-Methylpropyl)-3-oxa-2-thia-1-azaspiro[5.5]undecane-2,2-dioxide (Table 1, entry 6). Purified by chromatography on silica gel (9:1 hexanes/EtOAc); white solid: TLC R_f=0.64 (2:1 hexanes/EtOAc); ^1H NMR ($CDCl_3$, 400 MHz) δ 4.91 (dddd, 1H, J=11.7, 9.0, 4.3, 1.9 Hz), 3.73 (s, 1H), 2.51–2.42 (m, 1H), 1.92–1.82 (m, 1H), 1.77–1.57 (m, 5H), 1.52–1.28 (m, 7H), 1.34 (ddd, 1H, J=14.2, 8.5, 4.3 Hz), 0.95 (t, 3H, J=6.6 Hz), 0.93 (t, 3H, J=6.6 Hz) ppm; ^{13}C NMR ($CDCl_3$, 100 MHz) δ 78.7, 57.9, 44.2, 41.6, 40.5, 32.9, 25.6, 23.8, 22.8, 21.9, 21.1, 20.8 ppm; IR (thin film) ν 3254, 2934, 2864, 1447, 1419, 1386, 1347, 1278, 1188, 1158, 1104, 1061, 1028, 994, 974, 939, 877, 791 cm^{-1}; HRMS (ES^+) calcd for $C_{12}H_{23}NO_3S$ 261.1399, found 284.1304 (MNa^+).

4.3.1.9. 4,4-Dimethyl-6-(cyclohexylmethyl)tetrahydro-1,2,3-oxathiazine-2,2-dioxide (Table 1, entry 6). Purified by chromatography on silica gel (9:1 hexanes/EtOAc); white solid: TLC R_f=0.57 (2:1 hexanes/EtOAc); ^1H NMR ($CDCl_3$, 400 MHz) δ 4.93 (dddd, 1H, J=11.2, 9.0, 4.2, 2.3 Hz), 3.89 (s, 1H), 1.85–1.77 (m, 1H), 1.74–1.63 (m, 5H), 1.62–1.51 (m, 3H), 1.51 (s, 3H), 1.37 (ddd, 1H, J=14.0, 8.4, 4.1 Hz), 1.29 (s, 3H), 1.29–1.09 (m, 3H), 1.11–0.83 (m, 2H) ppm; ^{13}C NMR ($CDCl_3$, 100 MHz) δ 79.1, 55.8, 42.8, 41.9, 33.6, 33.0, 32.5, 31.9, 26.3, 26.1, 25.9, 25.1 ppm; IR (thin film) ν 3265, 2925, 2852, 1449, 1422, 1389, 1373, 1351, 1276, 1192, 1162, 1038, 1012, 944, 871, 801, 787 cm^{-1}; HRMS (ES^+) calcd for $C_{12}H_{23}NO_3S$ 261.1399, found 284.1292 (MNa^+).

4.3.1.10. 4,4-Dimethyl-5-(methoxymethyl)tetrahydro-1,2,3-oxathiazine-2,2-dioxide (Table 1, entry 7). Purified by chromatography on silica gel (gradient elution: 3:1→2:1 hexanes/EtOAc); clear oil: TLC R_f=0.47 (1:1 hexanes/EtOAc); ^1H NMR ($CDCl_3$, 400 MHz) δ 4.69 (dd, 1H, J=12.0, 4.0 Hz), 4.60 (dd, 1H, J=12.0, 8.7 Hz), 4.25 (br s, 1H), 3.48 (dd, 1H, J=9.6, 4.3 Hz), 3.34 (s, 3H), 3.27 (dd, 1H, J=9.6, 8.4 Hz), 2.03–1.96 (m, 1H), 1.41 (s, 3H), 1.35 (s, 3H) ppm; ^{13}C NMR ($CDCl_3$, 100 MHz) δ 71.2, 69.6, 59.2, 58.1, 42.6, 29.7, 29.4, 23.0 ppm; IR (thin film) ν 3270, 2922, 2851, 1465, 1426, 1391, 1357, 1225, 1185, 1162, 1112, 990, 928, 895, 794 cm^{-1}; HRMS (ES^+) calcd for $C_7H_{15}NO_4S$ 209.0722, found 232.0623 (MNa^+).

4.3.1.11. trans-4-Phenyl-5-(methoxymethyl)tetrahydro-1,2,3-oxathiazine-2,2-dioxide (Table 1, entry 8). Purified by chromatography on silica gel (4:1 hexanes/EtOAc); white solid: TLC R_f=0.51 (2:1 hexanes/EtOAc); ^1H NMR ($CDCl_3$, 400 MHz) δ 7.45–7.38 (m, 3H), 7.33–7.30 (m, 2H), 4.81 (t, 1H, J=11.7 Hz), 4.70 (dd, 1H, J=11.2, 8.6 Hz), 4.66 (dd, 1H, J=11.7, 4.7 Hz), 4.41 (br d, 1H, J=8.6 Hz), 3.17 (s, 3H), 3.13 (dd, 1H, J=9.8, 3.1 Hz), 3.01 (dd, 1H, J=9.8, 6.5 Hz), 2.50–2.40 (m, 1H) ppm; ^{13}C NMR ($CDCl_3$, 100 MHz) δ 136.7, 129.4, 129.3, 127.1, 74.7, 68.9, 61.1, 59.1, 39.8 ppm; IR (thin film) ν 3271, 2926, 1457, 1426, 1362, 1190, 1123, 1023, 973, 932, 880, 789 cm^{-1}; HRMS (ES^+) calcd for $C_{11}H_{15}NO_4S$ 257.0722, found 280.0624 (MNa^+).

4.3.1.12. 3-Oxa-2-thia-1-azabicyclo[5.1.0]octane-2,2-dioxide (Table 2, entry 1). Purified by chromatography on silica gel (gradient elution: 2:1→1:1 hexanes/EtOAc); clear oil: TLC R_f=0.26 (1:1 hexanes/EtOAc); ^1H NMR ($CDCl_3$, 400 MHz) δ 4.28–4.14 (m, 2H), 2.87–2.81 (m, 1H), 2.72 (d, 1H, J=5.2 Hz), 2.55–2.46 (m, 1H), 2.53 (d, 1H, J=5.2 Hz), 2.42–2.31 (m, 1H), 1.99–1.82 (m, 2H) ppm; ^{13}C NMR ($CDCl_3$, 100 MHz) δ 77.2, 71.3, 39.6, 26.6, 26.2 ppm.

4.3.1.13. 4-Ethenyltetrahydro-1,2,3-oxathiazine-2,2-dioxide (Table 2, entry 1). Clear oil: TLC R_f=0.52 (1:1 hexanes/EtOAc); ^1H NMR ($CDCl_3$, 400 MHz) δ 5.83 (ddd, 1H, J=17.3, 10.7, 4.9 Hz), 5.32 (dd, 1H, J=17.3, 1.8 Hz), 5.30 (dd, 1H, J=10.7, 1.7 Hz), 4.81–4.74 (m, 1H), 4.60–4.55 (m, 1H), 4.40–4.32 (m, 1H), 3.97 (br d, 1H, J=9.0 Hz), 1.90–1.84 (m, 2H) ppm; ^{13}C NMR ($CDCl_3$, 100 MHz) δ 134.9, 117.4, 71.6, 56.8, 29.2 ppm; IR (thin film) ν 3258, 2962, 2924, 2851, 1421, 1357, 1242, 1186, 1136, 1061, 1015, 988, 936, 864, 783 cm^{-1}; HRMS (ES^+) calcd for $C_5H_9NO_3S$ 163.0303, found 186.0199 (MNa^+).

4.3.1.14. trans-8-Methyl-3-oxa-2-thia-1-azabicyclo[5.1.0]octane-2,2-dioxide (Table 2, entry 2). Purified by chromatography on silica gel (gradient elution: 2:1→1:1 hexanes/EtOAc); clear oil: TLC R_f=0.26 (1:1 hexanes/EtOAc); ^1H NMR ($CDCl_3$, 400 MHz) δ 4.27–4.12 (m, 2H), 2.99 (dt, 1H, J=8.0, 4.0 Hz), 2.62–2.56 (m, 1H), 2.51–2.42 (m, 1H), 2.41–2.30 (m, 1H), 1.98–1.81 (m, 2H), 1.37 (d, 3H, J=6.3 Hz) ppm; ^{13}C NMR ($CDCl_3$, 100 MHz) δ 77.2, 71.2, 47.1, 26.9, 26.4, 17.0 ppm.

4.3.1.15. 4-((1E)-1-Propenyl)tetrahydro-1,2,3-oxathiazine-2,2-dioxide (Table 2, entry 2). Clear oil: TLC R_f=0.32 (2:1 hexanes/EtOAc); ^1H NMR ($CDCl_3$, 400 MHz) δ 5.83–5.73 (m, 1H), 5.47–5.39 (m, 1H), 4.75 (td, 1H, J=11.7, 3.2 Hz), 4.55 (ddd, 1H, J=11.7, 4.8, 1.9 Hz), 4.32–4.24 (m, 1H), 3.94 (br d, 1H, J=9.2 Hz), 1.92–1.86 (m, 2H), 1.73 (dt, 3H, J=6.6, 1.4 Hz) ppm; ^{13}C NMR ($CDCl_3$, 100 MHz) δ 129.4, 128.0, 71.6, 56.7, 29.7, 17.8 ppm; IR (thin film) ν 3260, 2922, 2853, 1421, 1355, 1236, 1186, 1130, 1077, 1049, 1010, 968, 936, 889, 864, 780 cm^{-1}; HRMS (ES^+) calcd for $C_6H_{11}NO_3S$ 177.0460, found 200.0355 (MNa^+).

4.3.1.16. cis-8-Methyl-3-oxa-2-thia-1-azabicyclo[5.1.0]octane-2,2-dioxide (Table 2, entry 3). Purified by chromatography on silica gel (gradient elution: 9:1→4:1 hexanes/EtOAc); clear oil: TLC R_f=0.43 (2:1 hexanes/EtOAc); ^1H NMR ($CDCl_3$, 400 MHz) δ 4.43 (dddd, 1H, J=11.9, 5.3, 1.8, 1.0 Hz), 4.30 (td, 1H, J=11.9, 3.6 Hz), 3.11 (quint, 1H, J=6.2 Hz), 2.83 (quint, 1H, J=5.3 Hz), 2.36–2.20 (m, 2H), 2.15–1.99 (m, 2H), 1.64 (d, 3H, J=6.4 Hz) ppm; ^{13}C NMR ($CDCl_3$, 100 MHz) δ 77.2, 71.9, 44.5, 26.0, 22.2, 9.2 ppm; IR (thin film) ν 2972, 2932, 1439, 1363, 1290, 1259, 1180, 1114, 1062, 1006, 983, 966, 916, 889, 847, 825, 761 cm^{-1}.

4.3.1.17. 4-((1Z)-1-Propenyl)tetrahydro-1,2,3-oxathiazine-2,2-dioxide (Table 2, entry 3). Clear oil: TLC R_f=0.75 (2:1 hexanes/EtOAc); ^1H NMR ($CDCl_3$, 400 MHz) δ 5.75 (dddd, 1H, J=14.0, 10.7, 7.0, 1.2 Hz), 5.24 (dddd, 1H, J=10.7, 8.0, 3.8, 1.8 Hz), 4.79 (ddd, 1H, J=12.8, 11.7, 2.5 Hz), 4.65–4.56 (m, 1H), 4.56 (ddd, 1H, J=11.7, 4.9, 1.5 Hz), 3.90 (br s, 1H), 1.93–1.81 (m, 1H), 1.75 (dt, 3H, J=7.0, 1.8 Hz), 1.75–1.69 (m,

1H) ppm; ^{13}C NMR ($CDCl_3$, 100 MHz) δ 130.7, 126.9, 71.8, 52.6, 29.9, 13.6 ppm; IR (thin film) ν 3242, 3027, 2980, 2923, 1432, 1349, 1239, 1187, 1171, 1090, 1061, 1026, 998, 944, 907, 866, 784 cm^{-1}; HRMS (ES^+) calcd for $C_6H_{11}NO_3S$ 177.0460, found 200.0358 (MNa^+).

4.3.1.18. 3-Oxa-2-thia-1-azabicyclo[6.1.0]nonane-2,2-dioxide (Table 2, entry 4). Purified by chromatography on silica gel (2:1 hexanes/EtOAc); clear oil: TLC R_f=0.37 (2:1 hexanes/EtOAc); ^{1}H NMR ($CDCl_3$, 400 MHz) δ 4.60 (ddd, 1H, J=12.8, 7.0, 3.0 Hz), 4.36 (ddd, 1H, J=12.8, 7.6, 3.4 Hz), 2.77 (d, 1H, J=6.7 Hz), 2.77–2.65 (m, 1H), 2.42 (d, 1H, J=4.9 Hz), 2.24–2.04 (m, 3H), 2.03–1.93 (m, 1H), 1.80–1.68 (m, 1H), 1.38–1.25 (m, 1H) ppm; ^{13}C NMR ($CDCl_3$, 100 MHz) δ 74.9, 42.4, 35.7, 28.9, 27.7, 25.6 ppm; IR (thin film) ν 3308, 2936, 2865, 1439, 1353, 1248, 1176, 1085, 1022, 968, 925, 865, 817 cm^{-1}; HRMS (ES^+) calcd for $C_6H_{11}NO_3S$ 177.0460, found 176.0372 (M^+-H).

4.3.1.19. 4,4-Dimethyl-6-(2-propen-1-yl)tetrahydro-1,2,3-oxathiazine-2,2-dioxide. Purified by chromatography on silica gel (gradient elution: 3:1→1: hexanes/EtOAc); clear oil: TLC R_f=0.51 (2:1 hexanes/EtOAc); ^{1}H NMR ($CDCl_3$, 400 MHz) δ 5.83–5.73 (m, 1H), 5.20–5.14 (m, 2H), 4.86 (ddd, 1H, J=11.4, 6.2, 2.4 Hz), 4.19 (br s, 1H), 2.56–2.48 (m, 1H), 2.44–2.36 (m, 1H), 1.66 (dd, 1H, J=14.3, 2.4 Hz), 1.58 (dd, 1H, J=14.3, 11.5 Hz), 1.49 (s, 3H), 1.30 (s, 3H) ppm; ^{13}C NMR ($CDCl_3$, 100 MHz) δ 131.4, 119.3, 80.0, 55.8, 40.7, 39.4, 31.8, 25.1 ppm; IR (thin film) ν 3268, 2979, 2926, 1423, 1390, 1374, 1351, 1192, 1157, 1015, 944, 925, 888, 871, 815, 785 cm^{-1}; HRMS (ES^+) calcd for $C_8H_{15}NO_3S$ 205.0773, found 228.0676 (MNa^+).

4.3.2. Characterization data for cyclopropyl clock experiment (Fig. 6)

4.3.2.1. (±)-3-(trans-2-Phenylcyclopropyl)propyl sulfamate. Purified by chromatography on silica gel (3:1 hexanes/EtOAc); white solid (69%): TLC R_f=0.21 (3:1 hexanes/EtOAc); ^{1}H NMR ($CDCl_3$, 400 MHz) δ 7.27–7.23 (m, 2H), 7.14 (tt, 1H, J=7.6, 1.2 Hz), 7.05–7.03 (m, 2H), 4.76 (br s, 2H), 4.26 (t, 2H, J=6.4 Hz), 1.94–1.87 (m, 2H), 1.68–1.63 (m, 1H), 1.61–1.44 (m, 2H), 1.07–0.99 (m, 1H), 0.93 (dt, 1H, J=8.4, 5.2 Hz), 0.79 (dt, 1H, J=8.4, 5.2 Hz) ppm; ^{13}C ($CDCl_3$, 100 MHz) δ 143.4, 128.3, 125.5, 125.4, 71.1, 30.2, 28.6, 23.2, 22.8, 16.1 ppm; IR (thin film) ν 3387, 3288, 2926, 1604, 1556, 1497, 1365, 1182, 937, 822, 751, 699 cm^{-1}.

4.3.2.2. (±)-4-(trans-2-Phenylcyclopropyl)tetrahydro-1,2,3-oxathiazine-2,2-dioxide. Reaction performed with 5 mol% $Rh_2(OAc)_2$. Purified by chromatography on silica gel (15:1 CH_2Cl_2/EtOAc); white solid (91%, 1:1 mixture of diastereomers by ^{1}H NMR). A single diastereomer of the product (stereochemistry unassigned) could be obtained by recrystallization from hexanes/EtOAc: TLC R_f=0.41 (CH_2Cl_2); ^{1}H NMR ($CDCl_3$, 400 MHz) δ 7.32–7.28 (m, 2H), 7.24–7.21 (m, 2H), 7.10–7.07 (m, 2H), 4.76–4.71 (m, 1H), 4.58 (dt, 1H, J=8.8, 2.8 Hz), 4.24 (d, 1H, J=7.6 Hz), 3.34–3.28 (m, 1H), 1.98–1.93 (m, 2H), 1.25–1.20 (m, 1H), 1.15 (dt, 1H, J=7.2, 4.4 Hz), 1.09 (dt, 1H, J=6.8, 4.4 Hz) ppm; ^{13}C NMR ($CDCl_3$, 100 MHz) δ 140.9, 128.5, 126.2, 125.9, 71.7, 60.0, 29.8, 26.6, 21.9, 13.7 ppm; IR (thin film) ν 3267, 1420, 1357, 1187, 1062, 1014, 941, 910, 861, 778 cm^{-1}.

4.4. Kinetic experiments

4.4.1. General procedure

Reactions were conducted in anhydrous CH_2Cl_2 distilled from CaH_2 and stored over activated 4 Å molecular sieves or dried by passage through activated alumina columns under 12 psi of N_2. Standard solutions of reagents in CH_2Cl_2 were stored in Schlenk flasks at −20 °C to minimize solvent evaporation. $PhI(OAc)_2$ was obtained from Acros Chemical Company and all experiments employed oxidant from the same lot number. Dimeric Rh-tetracarboxylates were desolvated immediately prior to use by heating solid samples to 90 °C under reduced pressures (~1 Torr) for 2 h. Sulfamate substrates were dried azeotropically with benzene and stored under vacuum. Product conversion was determined by integration of the ^{1}H NMR spectra. Maximum product concentration was fixed at 0.157 M (=initial concentration of sulfamate ester). Standard reactant concentrations were chosen to match those used in the general protocol for the preparation of oxathiazinanes (vide supra):

[sulfamate ester]=0.157 M in CH_2Cl_2 or CD_2Cl_2
[$Rh_2(O_2CCMe_3)_4$]=3.14 mM in CH_2Cl_2 or CD_2Cl_2 (0.02×sulfamate ester concentration)
[$PhI(OAc)_2$]=0.173 M in CH_2Cl_2 or CD_2Cl_2 (1.1×sulfamate ester concentration)

4.4.2. ^{1}H NMR method for determining product conversions

Magnesium oxide was omitted from these experiments. To determine the rates of product formation at the standard reactant concentrations, a CD_2Cl_2 solution of isoamyl sulfamate and $Rh_2(O_2C^tBu)_4$ (0.314 M and 6.28 mM, respectively) and a CD_2Cl_2 solution of $PhI(OAc)_2$ (0.346 M) were prepared; 300 μL of each solution was co-injected into a Pyrex NMR tube at 23 °C and the ^{1}H NMR spectrum was immediately acquired. The NMR probe temperature was maintained at 22.6 °C. Reaction progress was monitored by periodic ^{1}H NMR acquisition.

4.4.3. Sample analysis method for determining product conversion

The use of MgO was compatible with kinetic analysis performed under these conditions; however, in order to have a direct comparison to results from the ^{1}H NMR experiments, MgO was typically omitted. Aliquots (100 μL) were removed periodically from the reaction mixture and injected into a rapidly stirring mixture of 1.0 mL of 1.0 M aqueous $Na_2S_2O_3$ and 1.0 mL of CH_3CN. EtOAc was added (5 mL) and the organic portion was collected and concentrated under reduced pressure. The isolated material was dissolved in $CDCl_3$ and the product ratio was determined by integration of the ^{1}H NMR spectrum or by integration of the HPLC chromatogram.

4.4.4. Pseudo-first-order kinetics experiments to determine the rate dependence on [PhI(OAc)$_2$]

Product concentration was determined by analyzing sample aliquots taken at intermediate time points. Reactant concentrations were taken as follows and correspond to the reactant concentrations and equivalencies employed in the general protocol for the preparation of oxathiazinanes except the sulfamate concentration is 10 times that of a standard reaction (9 equiv compared to oxidant) (vide supra):

[sulfamate ester]=1.57 M in CH_2Cl_2 (9.0×$PhI(OAc)_2$ concentration)
[$Rh_2(O_2CCMe_3)_4$]=7.85 mM in CH_2Cl_2 (0.045×$PhI(OAc)_2$ concentration)
[$PhI(OAc)_2$]=0.173 M in CH_2Cl_2

Acknowledgements

We would like to thank the many authors who have contributed to this commemorative issue and the awards committee for their gracious acknowledgement of our work. We are indebted to our colleague, John Brauman, for many stimulating discussions and his insightful analysis and to a reviewer for a deep and scholarly analysis of our submitted draft. K.W.F. is grateful to both the National Science Foundation and Amgen for fellowship support. C.G.E. is grateful to both the National Science Foundation and the American Chemical Society Organic Division for fellowship support. B.H.B. was the recipient of an Eli Lilly graduate fellowship award.

The National Science Foundation, the National Institutes of Health, Amgen, Boehringer-Ingelheim, GlaxoSmithKline, Merck, and Pfizer are acknowledged for their generous support of this work.

References and notes

1. For reviews on C–H amination, see: (a) Espino, C. G.; Du Bois, J. In *Modern Rhodium-Catalyzed Organic Reactions*; Evans, P. A., Ed.; Wiley-VCH: Weinheim, 2005; pp 379–416; (b) Dauban, P.; Dodd, R. H. *Synlett* **2003**, 1571–1586; (c) Müller, P.; Fruit, C. *Chem. Rev.* **2003**, *103*, 2905–2920; (d) Halfen, J. A. *Curr. Org. Chem.* **2005**, *9*, 657–669; (e) Lebel, H.; Leogane, O.; Huard, K.; Lectard, S. *Pure Appl. Chem.* **2006**, *78*, 363–375; (f) Li, Z. G.; He, C. *Eur. J. Org. Chem.* **2006**, 4313–4322; (g) Davies, H. M. L. *Angew. Chem., Int. Ed.* **2006**, *45*, 6422–6425; (h) Davies, H. M. L.; Manning, J. R. *Nature* **2008**, *451*, 417–424; (i) Díaz-Requejo, M. M.; Pérez, P. J. *Chem. Rev.* **2008**, *108*, 3379–3394.
2. Recent, representative examples include: (a) Liang, J.-L.; Yuan, S.-X.; Huang, J.-S.; Yu, W.-Y.; Che, C.-M. *Angew. Chem., Int. Ed.* **2002**, *41*, 3465–3468; (b) Fiori, K. W.; Fleming, J. J.; Du Bois, J. *Angew. Chem., Int. Ed.* **2004**, *43*, 4349–4352; (c) Fruit, C.; Müller, P. *Tetrahedron: Asymmetry* **2004**, *15*, 1019–1026; (d) Cui, Y.; He, C. *Angew. Chem., Int. Ed.* **2004**, *43*, 4210–4212; (e) Espino, C. G.; Fiori, K. W.; Kim, M.; Du Bois, J. *J. Am. Chem. Soc.* **2004**, *126*, 15378–15379; (f) Lebel, H.; Huard, K.; Lectard, S. *J. Am. Chem. Soc.* **2005**, *127*, 14198–14199; (g) Kim, M.; Mulcahy, J. V.; Espino, C. G.; Du Bois, J. *Org. Lett.* **2006**, *8*, 1073–1076.
3. For some examples of C–H amination in natural product synthesis, see: (a) Wehn, P. M.; Du Bois, J. *J. Am. Chem. Soc.* **2002**, *124*, 12950–12951; (b) Trost, B. M.; Gunzner, J. L.; Dirat, O.; Rhee, Y. H. *J. Am. Chem. Soc.* **2002**, *124*, 10396–10415; (c) Huang, H.; Panek, J. S. *Org. Lett.* **2003**, *5*, 1991–1993; (d) Parker, K. A.; Chang, W. S. *Org. Lett.* **2003**, *5*, 3891–3893; (e) Hinman, A.; Du Bois, J. *J. Am. Chem. Soc.* **2003**, *125*, 11510–11511; (f) Fleming, J. J.; Du Bois, J. *J. Am. Chem. Soc.* **2006**, *128*, 3926–3927.
4. Fiori, K. W.; Du Bois, J. *J. Am. Chem. Soc.* **2007**, *129*, 562–568.
5. For related mechanistic studies, see: (a) Nägeli, I.; Baud, C.; Bernardinelli, G.; Jacquier, Y.; Moran, M.; Müller, P. *Helv. Chim. Acta* **1997**, *80*, 1087–1105; (b) Müller, P.; Baud, C.; Nägeli, I. *J. Phys. Org. Chem.* **1998**, *11*, 597–601; (c) Au, S.-M.; Huang, J.-S.; Yu, W.-Y.; Fung, W.-H.; Che, C.-M. *J. Am. Chem. Soc.* **1999**, *121*, 9120–9132; (d) Liang, J.-L.; Yuan, S.-X.; Huang, J.-S.; Che, C.-M. *J. Org. Chem.* **2004**, *69*, 3610–3619; (e) Leung, S. K.-Y.; Tsui, W.-M.; Huang, J.-S.; Che, C.-M.; Liang, J.-L.; Zhu, N. *J. Am. Chem. Soc.* **2005**, *127*, 11629–16640; (f) Badiei, Y. M.; Krishnaswamy, A.; Melzer, M. M.; Warren, T. H. *J. Am. Chem. Soc.* **2006**, *128*, 15056–15057; (g) Huard, K.; Lebel, H. *Chem.—Eur. J.* **2008**, *14*, 6222–6230.
6. Du Bois, J. *CHEMTRACTS—Org. Chem.* **2005**, *18*, 1–13.
7. Impressive examples of Rh-catalyzed intermolecular C–H amination have also appeared, see Ref. 4: (a) Liang, C.; Robert-Peillard, F.; Fruit, C.; Müller, P.; Dodd, R. H.; Dauban, P. *Angew. Chem., Int. Ed.* **2006**, *45*, 4641–4644; (b) Liang, C.; Fruit, C.; Robert-Peillard, F.; Müller, P.; Dodd, R. H.; Dauban, P. *J. Am. Chem. Soc.* **2008**, *130*, 343–350.
8. Espino, C. G.; Du Bois, J. *Angew. Chem., Int. Ed.* **2001**, *40*, 598–600.
9. For general reviews, see: (a) Doyle, M. P.; McKervey, M. A.; Ye, T. *Modern Catalytic Methods for Organic Synthesis with Diazo Compounds: From Cyclopropanes to Ylides*; Wiley and Sons: New York, NY, 1997; (b) Davies, H. M. L.; Beckwith, E. J. *Chem. Rev.* **2003**, *103*, 2861–2904; (c) Doyle, M. P. *J. Org. Chem.* **2006**, *71*, 9253–9260.
10. (a) Nakamura, E.; Yoshikai, N.; Yamanaka, M. *J. Am. Chem. Soc.* **2002**, *124*, 7181–7192; (b) Nowlan, D. T., III; Gregg, T. M.; Davies, H. M. L.; Singleton, D. A. *J. Am. Chem. Soc.* **2003**, *125*, 15902–15911; (c) Wong, F. M.; Wang, J.; Hengge, A. C.; Wu, W. *Org. Lett.* **2007**, *9*, 1663–1665.
11. For general discussions on mechanisms of C–H oxidation, see: (a) Newcomb, M.; Toy, P. H. *Acc. Chem. Res.* **2000**, *33*, 449–455; (b) Groves, J. T. *J. Inorg. Biochem.* **2006**, *100*, 434–447.
12. $Rh_2(esp)_2$=Rh_2(α,α,α′,α′-tetramethyl-1,3-benzenedipropionate)$_2$, see Ref. 2e. This catalyst may be purchased from Aldrich Chemical Company.
13. $Rh_2(O_2CCPh_3)_4$ was first described by Ikegami, see: Hashimoto, S.-i.; Watanabe, N.; Ikegami, S. *Tetrahedron Lett.* **1992**, *33*, 2709–2712.
14. For a leading reference on selectivity influences caused by ligands on dirhodium(II) complexes, see: Doyle, M. P.; Ren, T. *Prog. Inorg. Chem.* **2001**, *49*, 113–168.
15. Related observations have been noted by Che in reactions catalyzed by Ru–porphyrin complexes, see Ref. 5c.
16. An increased preference for 3° over benzylic C–H insertion was noted in diazoalkane reactions promoted by $Rh_2(O_2CCPh_3)_4$, see: Taber, D. F.; Joshi, P. V. *J. Org. Chem.* **2004**, *69*, 4276–4278.
17. In some cases, $Rh_2(O_2CCPh_3)_4$ has been found to influence adversely diastereoselective sulfamate ester insertions. For examples of diastereoselective sulfamate oxidation reactions, see: Wehn, P. M.; Lee, J.; Du Bois, J. *Org. Lett.* **2003**, *5*, 4823–4826.
18. For Rh-catalyzed alkene aziridination, see: (a) Müller, P.; Baud, C.; Jacquier, Y. *Can. J. Chem.* **1998**, *76*, 738–750; (b) Fruit, C.; Robert-Peillard, F.; Bernardinelli, G.; Müller, P.; Dauban, P.; Dodd, R. H. *Tetrahedron: Asymmetry* **2005**, *16*, 3484–3487; (c) Bodner, R.; Marcellino, B. K.; Severino, A.; Smenton, A. L.; Rojas, C. M. *J. Org. Chem.* **2005**, *70*, 3988–3996; (d) Guthikonda, K.; Wehn, P. M.; Caliando, B. J.; Du Bois, J. *Tetrahedron* **2006**, *62*, 11331–11342 and Ref. 2f.
19. For examples of catalysts that strongly favor allylic C–H insertion, see: (a) Zalatan, D. N.; Du Bois, J. *J. Am. Chem. Soc.* **2008**, *130*, 9220–9221; (b) Milczek, E.; Boudet, N.; Blakey, S. *Angew. Chem., Int. Ed.* **2008**, *47*, 6825–6828.
20. A related bicyclic structure has been prepared previously, see: Wehn, P. M.; Du Bois, J. *Org. Lett.* **2005**, *7*, 4685–4688 and Ref. 2c.
21. A similar strategy was used to perform a Hammett analysis of Rh-catalyzed carbene C–H insertion, see: Wang, J.; Chen, B.; Bao, J. *J. Org. Chem.* **1998**, *63*, 1853–1862.
22. We have found that $Rh_2(OAc)_4$ and $Rh_2(oct)_4$ may be used interchangeably with no consequence to product yields or selectivities.
23. This ρ-value was obtained by plotting $\log(k_{Ar}/k_{Ph})$ versus σ^+ (R^2=0.9575). Plotting this data versus σ_p gives an R^2 of 0.9113.
24. (a) Lowry, T. H.; Richardson, K. S. *Mechanism and Theory in Organic Chemistry*, 3rd ed.; Harper & Row: New York, NY, 1987; pp 143–154; (b) Hansch, C.; Leo, A.; Taft, R. W. *Chem. Rev.* **1991**, *91*, 165–195.
25. Davies, H. M. L.; Jin, Q.; Ren, P.; Kovalevsky, A. Y. *J. Org. Chem.* **2002**, *67*, 4165–4169.
26. The ^{13}C NMR spectrum was acquired using a relaxation delay of 5 s. This method for determining the ratio of isotopomers has been utilized by Wang and Adams, see Ref. 27a.
27. (a) Wang, P.; Adams, J. *J. Am. Chem. Soc.* **1994**, *116*, 3296–3305; (b) Davies, H. M. L.; Hansen, T.; Churchill, M. R. *J. Am. Chem. Soc.* **2000**, *122*, 3063–3070.
28. Lwowski, W.; Maricich, T. J. *J. Am. Chem. Soc.* **1965**, *87*, 3630–3637.
29. Au, S.-M.; Huang, J.-S.; Che, C.-M.; Yu, W.-Y. *J. Org. Chem.* **2000**, *65*, 7858–7864.
30. Lin, X.; Zhao, C.; Che, C.-M.; Ke, Z.; Phillips, D. L. *Chem. Asian J.* **2007**, *2*, 1101–1108; Also, see: Lin, X.; Che, C.-M.; Phillips, D. L. *J. Org. Chem.* **2008**, *73*, 529–537.
31. (a) Lwowski, W. In *Nitrenes*; Lwowski, W., Ed.; Interscience: New York, NY, 1970; pp 185–224; (b) Terashima, S.; Yamada, S.-i. *Chem. Pharm. Bull.* **1968**, *16*, 1953–1971; Also, see: Liu, J.; Mandel, S.; Hadad, C. M.; Platz, M. S. *J. Org. Chem.* **2004**, *69*, 8583–8593.
32. For a recent analysis of Cu(I)-promoted C–H amination, see: Badiei, Y. M.; Dinescu, A.; Dai, X.; Palomino, R. M.; Heinemann, F. W.; Cundari, T. R.; Warren, T. H. *Angew. Chem., Int. Ed.* **2008**, *47*, 9961–9964 and references therein.
33. Müller has performed an analogous intermolecular amination reaction using NsN=IPh, catalytic $Rh_2(OAc)_4$, and a cyclopropane clock that ring-opens with a rate constant of 2×10^{10} s^{-1}, see Ref. 5a.
34. Simakov, P. A.; Choi, S.-Y.; Newcomb, M. *Tetrahedron Lett.* **1998**, *39*, 8187–8190.
35. Choi, S.-Y.; Toy, P. H.; Newcomb, M. *J. Org. Chem.* **1998**, *63*, 8609–8613.
36. It is difficult to establish the precise role for MgO in the amination reaction due to its insolubility in CH_2Cl_2 and C_6H_6. In its presence, we have observed a diminution in the initial rate of product formation (as determined by HPLC analysis of reaction aliquots). In its absence, we have noted that $PhI(OAc)_2$ is consumed more rapidly than oxathiazinane product is formed.
37. We have attempted to lower the catalyst loadings below 0.1 mol % in order to observe a rate influence on catalyst concentration. At such low catalyst loadings, the product is not formed at appreciable levels.
38. Under standard conditions the substrate concentration is 0.157 M.
39. Iminoiodinane **15** was employed for these studies as it is more easily prepared and isolated than iminoiodinanes derived from other sulfamate starting materials.
40. ^1H NMR experiments with $PhI(OAc)_2$ and carbamate esters also show no apparent reaction between these starting materials.
41. A control experiment with $PhI(OAc)_2$ and 1,1,1-trichloro-4-phenylbutan-2-yl sulfamate shows ~10% of the corresponding iminoiodinane. A similar observation has been noted with 2,2,2-trichloroethylsulfamate, see Ref. 4.
42. Intermolecular C–H amination experiments involving the kinetic resolution of chiral sulfonimidamides support the idea of reversible iodoimine formation, see Ref. 7b.
43. Espino, C. G. Ph.D. Thesis, Stanford University, Stanford, CA, 2004.